Entropy Production and Annihilation in Quantum Feedback Protocols

J. T. Monroe[1]

[1]*Department of Physics, Washington University, St. Louis, Missouri 63130*

(Dated: May 16, 2018)

In this experiment we investigate the paradox of how time-reversible dynamics can produce time-irreversible processes such as entropy production. We study individual quantum trajectories and compare forward and backward path probabilities to infer a net preference for a statistical arrow of time quantified by an entropy measure. Moreover, we implement post-selected feedback protocols wherein the extraction and subsequent use of information seems to set a definite preference for the direction of time. Though causal-order feedback does not effect entropy production, a reversed causal order feedback protocol does reverse the flow of entropy, annihilating rather than creating entropy, revealing the essential role of causality is the direction of the arrow of time.

I. INTRODUCTION

Standard dynamics of quantum systems, as governed by Schrödinger's equation, are time-reversal invariant. Taking $t \to -t$ and taking the complex conjugate [1] leaves $i\hbar\frac{\partial}{\partial_t}\psi(t) = H\psi(t) \to (-)i\hbar\frac{\partial}{\partial_(-t)}\psi(t) = \hat{H}\psi(t)$ unchanged. While under such dynamics the von Neumann entropy is constant many quantum mechanical systems allow for the gain or loss of information corresponding to changes in von Neumann entropy. For example, the many-to-one mapping of projective measurement breaks time-reversal symmetry and changes the entropy. Moreover, decoherence resulting from a loss of information produces mixed states with maximal entropy, while entanglement injects correlations into the density matrix thereby decreasing entropy [2].

Each of these phenomena displays entropy production or annihilation. However, systems described by unitary (i.e. norm-preserving) dynamics can have no such entropy change. This is the quantum analogue of Loschmidt's paradox wherein phase-space volume conservation (as guaranteed by Louiville's theorem) seemingly cannot produce phase space enlarging processes, as demanded by the second law of thermodynamics.

Changes in the von Nuemann entropy arise in quantum dynamics when information is incomplete. That is, one must distinguish between a system which is completely known and an environment which is largely unknown. Such a treatment allows the universe to undergo (unknown) unitary evolution, while the system can locally increase (or decrease) its entropy. This open quantum system formalism yields stochastic system evolution which obeys more nuanced laws of entropy production. Rather than satisfying Clausius' maxim that (thermodynamic) entropy must always be maximized, statistical entropy of open quantum systems can fluctuate between positive and negative values, especially far from equilibrium. When the environment can be monitored with high efficiency the system's lost information can be captured and the stochastic evolution can be directly reconstructed.

The details of these fluctuations have proved remarkably fruitful in resolving the classical Loschmidt paradox [3]. Here, paradigmatic colloidal particles undergo Brownian motion, and their continuous trajectories are classified as entropy producing or entropy annihilating based on the relative probability of moving forward or backward in time. These entropy relations entail a variety of generalized, non-equilibrium thermodynamic laws [4].

However, in textbook quantum mechanics, recording trajectories by continuously monitoring quantum states is not allowed. To measure a state is to collapse it to the eigenstate of the recorded eigenvalue. However, the formalism of positive-operator valued measures (POVMs) allows for continuous, weak measurement via coupling to ancillary systems[5]. The ancilla coupling partially encodes qubit information into ancilla degrees of freedom so that ancilla measurements only partially disturb the system. Thus continuous trajectories of a quantum system can be measured, and forward and backward path probabilities can be calculated, allowing for a characterization of the entropy production (and annihilation) in open quantum systems.

To do so, one must begin with reversible equations of motion [4]. Such reversible measurement dynamics are enabled by the positivity of the POVM mapping [6]. For a measurement of non-zero strength some backaction will be imparted on the system. After collecting a record value, r, the initial density matrix ρ_1 updates $\rho_1 \to M_r\rho_0 M_r^\dagger$ for a probabilistic POVM, M_r. This stochastic update protocol is reversible since we may apply a time-reversed measurement, $\tilde{M}_{r_1} = \Theta M_{r_1}\Theta^\dagger$, to get a reversed trajectory:

$$\tilde{\rho}_1 = \tilde{M}_{r_1}\rho_1\tilde{M}_{r_1}^\dagger \tag{1a}$$

$$= \tilde{M}_{r_1}\left(M_{r_1}\rho_0 M_{r_1}^\dagger\right)\tilde{M}_{r_1}^\dagger \tag{1b}$$

where we have applied the so-called "active" transformation by reversing the state resulting from n measurements in the forward direction and by applying measurement operators in reverse order. Given that $\tilde{M}_{r_n}\tilde{M}_{r_n}^\dagger = \hat{\mathcal{I}}$, this reduces to $\tilde{\rho}_0 = \Theta\rho_0\Theta^\dagger$, the time-reversed initial state. Thus, because we track the individual record steps, r_n,

we can apply time-reversed measurement operators to reverse the dynamics of measurement.

With individual quantum trajectories and reversal probabilities we may proceed with calculating a generalized entropy:

$$Q \equiv \ln\left[\frac{P_F}{P_B}\right] \tag{2}$$

where P_F and P_B are the probabilities of a trajectory moving forward or backward in time, respectively. This definition of entropy has offered insights into a statistical arrow of time [7], and leads to a generalization of the second law by means of a detailed fluctuation theorem [8]:

$$\frac{P(+Q)}{P(-Q)} = e^{Q} \tag{3}$$

Such a remarkable, exact equality characterizes much more than the (generally false) statement about the maximization of entropy. It not only allows for negative entropy fluctuations, but requires at least small negative entropy fluctuations to balance the average. The apparent absence of entropy annihilation changes arises from the exponential suppression of backward trajectories for long times and large system sizes. The foundation of the fluctuation theorem is essentially causal ordering: because causes precede effects forwards moving trajectories are more probably than backwards moving [9].

In the main result of this paper we investigate the statistical arrow of time and its corresponding fluctuation theorem within the context of casual and anti-causal ordered feedback protocols (COF and ACOF). Because feedback typically entails receiving information *before* using it, feedback protocols impart a definite direction of time. Moreover, if the feedback process is ACOF, one would expect time to flow backward: effecting the system *before* it's cause is processed. We show that ACOF protocols reverse the arrow of time, however, COF protocols do not impart any changes compared to arrow of time measurements without feedback. By interpreting the arrow of time as a statement of the second law of thermodynamics, we highlight the causal origins of the second law— when information from the future is used to feedback the past, entropy decreases, heat flows from cold to hot and the arrow of time moves backwards [9].

II. RESULTS

Our experiment consists of an artificial atom coupled to the electromagnetic field. The atom is realized by the two lowest levels of a superconducting transmon circuit, and it is dispersively coupled to a single electromagnetic mode of an aluminum cavity cooled in a dilution refrigerator to a temperature of 10 mK. To infer the state of the qubit, coherent states are transmitted through the cavity. They receive a qubit-state-dependent frequency shift according to the dispersive Jaynes-Cummings Hamiltonian: $H_{\rm JC}/\hbar = \frac{\omega_q}{2}\sigma_z + \hat{a}^\dagger\hat{a}(\omega_c + \chi\sigma_z)$ where the dispersive interaction, $H_{\rm int} = \chi\hat{a}^\dagger\hat{a}\sigma_z$, has been interpreted as a qubit-state-dependent frequency shift on the cavity, and the Lamb shift has been incorporated into the qubit frequency. The quadrature component of the phase-shifted cavity tone is composed of Gaussian distributions for each qubit state with (equal) variance σ^2 and means separated by ΔV [Figure 1].

The cavity-qubit coupling enables qubit state inference, but also induces backaction on the qubit. The dynamics of this disturbance are modeled with Gaussian POVMs according to measurement operators: $\hat{M}_{V_m} = \frac{1}{\sqrt[4]{2\pi\sigma^2}}\exp\left[-(V_m-1)^2/2\sigma^2\right]$. These operators dictate how to update the density matrix, ρ, according to measured voltages, V_m: $\rho \to \mathcal{N} M_{V_m}\rho M_{V_m}^\dagger$. We can also directly calculate expectation values of Pauli operators, $\langle\sigma_{x_i}\rangle = \mathrm{Tr}\left[\rho\sigma_{x_i}\right]$, to ascertain measurement-update equations for Bloch coordinates[10]:

$$Z_{V_m} = \tanh\left[\frac{V_m S}{2\Delta V}\right] \tag{4a}$$

$$X_{V_m} = \sqrt{1 - Z_{V_m}^2}\, e^{-\gamma\tau} \tag{4b}$$

where $\gamma = \frac{8\chi^2(1-\eta)\bar{n}}{\kappa} = 2.54$ MHz is the dephasing rate.

The separation parameter, $S \equiv \frac{\Delta V^2}{\sigma^2}$, directly quantifies the backaction on the qubit based on the cavity tone strength. It can be expressed as $S = \frac{64\chi^2\bar{n}\eta}{\kappa}\tau$ [11], where $\chi/2\pi = -0.25$ MHz is the dispersive shift, $\bar{n}$ is the (tunable) intra-cavity photon number, $\eta = 0.31$ is the quantum efficiency, $\kappa/2\pi = 3.37$ MHz is the cavity linewidth, and $\tau = 145$ ns is the measurement duration. When $S = 3$ the qubit states are well-separated, seen in Figure 1a and we have strong qubit-state inference, thereby projecting the qubit into an eigenstate. On the other hand, decreasing the intra-cavity photon number, $\bar{n}$, so that $S = 0.4$ induces much smaller measurement-backaction on the qubit (Figure 1b) while still providing partial information about the updated qubit state, providing a weak measurement.

In Figure 1c we show that our measurement-update equations, Equation 4, accurately predict the measured state. For $1.3 \cdot 10^6$ experimental runs we collect a weak measurement voltage, V_m, followed by a projective measurement. We then bin trajectories based on V_m and compare the bin's average value of $\langle Z\rangle$ with the predicted Z_{V_m}. Likewise for $\langle X\rangle$ and $\langle Y\rangle$. Figure 1c's good agreement implies that our scheme for weak measurement faithfully reproduces individual quantum trajectories.

We now turn to calculating the probability of individual trajectories in order to infer whether they are likely moving forwards or backwards in time. Within

the POVM formalism, the probability of a measurement outcome V_m is $P(V_m) = \mathrm{Tr}\left[M_{V_m}\rho\right]$. In order to directly compare forward and backward probabilities we condition on the time-sensitive initial condition. We reverse trajectories in the so-called "active transformation" where coordinates and ordering of measurement outcomes are reversed, while the sign of the measurement is fixed. With these paradigms we calculate the forward and backward path probabilities via conditioned Bayesian inference:

$$P_F(V_m|z) = \tfrac{1+z}{2} e^{-\frac{(V_m - V_{\mathrm{gnd}})^2 S}{2\Delta V^2}} + \tfrac{1-z}{2} e^{-\frac{(V_m - V_{\mathrm{ex}})^2 S}{2\Delta V^2}} \tag{5a}$$

$$P_B(V_m|\tilde{z}_t) = \tfrac{1+\tilde{z}_t}{2} e^{-\frac{(V_m - V_{\mathrm{gnd}})^2 S}{2\Delta V^2}} + \tfrac{1-\tilde{z}_t}{2} e^{-\frac{(V_m - V_{\mathrm{ex}})^2 S}{2\Delta V^2}} \tag{5b}$$

where $\Delta V = V_{\mathrm{gnd}} - V_{\mathrm{ex}}$ for mean voltages associated with ground and excited states, and $\tilde{z}_t$ is the Bloch coordinate propagated to time t and then time-reversed.

With such forward and backward probabilities for individual quantum trajectories we can estimate the statistical arrow of time from the log ratio of forward and backward probabilities

$$Q \equiv \ln\left[\frac{P_F(V_m)}{P_B(V_m)}\right] \tag{6}$$

which in general is non-zero. The preference for forward-moving trajectories comes from the preponderance of measurement to project towards eigenstates. As the measurement dynamics unfold, previous voltages induce backaction towards one or the other poles causing the the relative weights of Equation 5 to favor continued progression towards that eigenstate. Moreover, initial conditions set a perference for a these weights to further heighten the movement towards an eigenstate. Thus, despite the reversibility of individual measurements we nonetheless infer a preference for $\bar{Q} > 0$ (forward in time).

We now turn to our feedback protocol for state stabilization. The goal of the feedback is to maintain an initial state, here $|+x\rangle$, in the face of decoherence and stochastic evolution from environmental interactions. Due to imperfect quantum efficiency our recorded trajectories are effectively averaged over alternative trajectories, resulting in irrevocable measurement-induced decoherence. In order to isolate the effect of feedback on the arrow of time we define pure state trajectories as our recorded trajectories, and deduce measurement-induced dephasing via the average over our collected ensemble. In this paradigm successful feedback involves purifying beyond this ensemble to a purity consistent with the average purity of individual trajectories, allowing an investigation of the arrow of time in an effectively frictionless system.

Furthermore, to explore the nature of ACOF we implement this feedback protocol with a post-selection

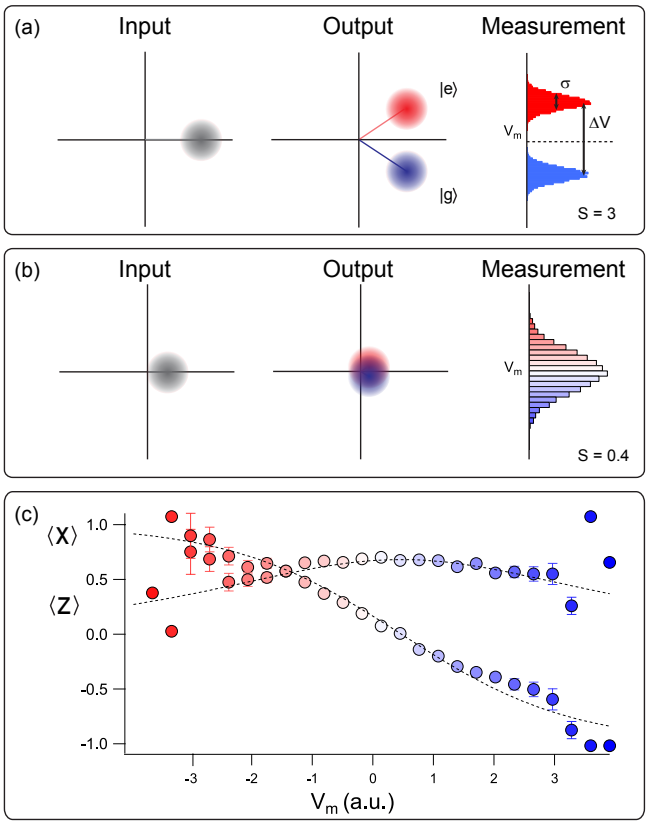

Figure 1: Our experimental readout scheme involves (**a**) a coherent tone sent into the cavity which receives a qubit-state dependent phase shift resulting in two well-separated Gaussian distributions (S=3). (**b**) Conversely, we implement weak measurement by decreasing the intra-cavity photon number so that the qubit states do not resolve (S=0.4). (**c**) Instead, Bayesian state update (Equation 4) enables faithful state reconstruction via tomographic outcomes conditioned on averaged homodyne voltages. $\langle y\rangle$ is not shown, but is consistent with zero, as expected for σ_y rotation.

method, pictured in Figure 2. After preparing the target state, we allow the qubit to stochastically evolve while monitoring its state. We then apply a corrective rotation pulse, θ_{app}, about the y-axis with a randomly chosen angle between $-\frac{\pi}{4}$ and $\frac{\pi}{4}$. In post-analysis we select realizations wherein we "guessed" the ideal feedback angle, $\theta_{\mathrm{ideal}} = \tan^{-1}\left[\frac{Z_{V_m}}{X_{V_m}}\right]$, within $\frac{\pi}{20}$.

In this feedback protocol we then evaluate forward and backward probabilities of individual trajectories. Critically, the backwards probability, $P_B(V_m|\tilde{z}_t)$ is based on the time-reversed coordinate after the time-reversed feedback (Figure 2). At this stage the state has undergone both feedback and its time-reversal, effectively canceling the effect of feedback [12]. Thus in the case of causal order feedback, the arrow of time ratio, seen in Figure 3, is the same as if we had not applied feedback. Our results

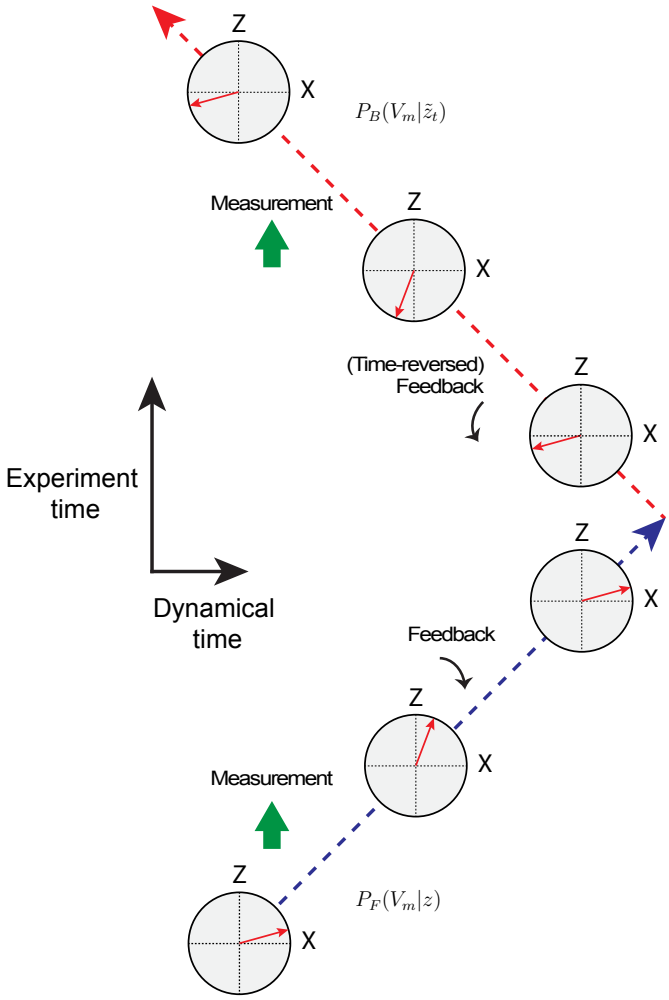

Figure 2: Our feedback experiments entail stabilizing an initial state and comparing forward and backward path probabilities. Experimental realizations involve first preparing a state which is then perturbed by measurement-induced backaction. We apply a corrective unitary feedback rotation to return (ideally) to the initial state. In order to compare to the reversed case, we flip the dynamics of the system (in analysis), applying the time-reversed unitary feedback (negative angle) before calculating the measurement probability according to Equation 5. The backaction of the forward measurement outcome restores the system to the time-reverse of the initial state.

for forward feedback are consistent with previous studies [7, 13].

What becomes of feedback in reversed causal order? Here we utilize the same feedback mechanism, but after state preparation we proceed with a random rotation succeeded by measurement. Interpreted as a feedback protocol, we correct the state and then measure to see what feedback should be applied. With this protocol we observe a backwards arrow of time, seen in Figure 3, reflecting the anticausal order of the "feedback". In one

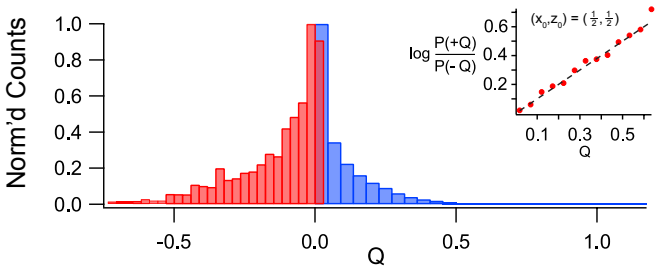

Figure 3: Histogram of the log ratio of forward and backward probabilities, Q (Equation 6), calculated from individual quantum trajectories. In standard COF (blue) the trajectories are essentially all entropy-producing due to the initial state, $|+x\rangle$. Conversely, for ACOF (red), time apparently flows backwards due to the imposed anticausality. The figure inset shows a preliminary validation of the fluctuation theorem for a different initial condition: $|\psi_0\rangle = \left(\sqrt{3}\,|g\rangle + |e\rangle\right)/2$.

sense, the measurements which correctly "unmeasure" the rotation are so exceedingly rare that an ensemble consisting of these trajectories must annihilate entropy. In another sense, because the arrow of time is a fundamentally causal relationship, an ACOF protocol produces an "anti-natural" arrow of time.

We could, in principal, use this data to verify the detailed fluctuation theorem (Equation 3). However, as Figure 3 shows, the occurrence of entropy annihilating trajectories are exceedingly rare for states prepared in $|+x\rangle$. For a given value of entropy production $+Q$, we cannot measure the probability of $-Q$, and therefore cannot verify Equation 3. However, for preliminary data of a different initial condition, $(x_0,z_0) = (0.5, 0.5)$, we find that the entropy production and annihilation do balance according to the detailed fluctuation theorem (Figure 3, inset).

III. CONCLUSION

In this experiment we have investigated the nuance of entropy production (and annihilation) in quantum systems. The details of such processes require a microscopic view of individual trajectories, and an ability to evaluate probabilities of trajectories moving forwards and backwards in time.

Insights into the foundation of generalized second laws have pointed to causality as a pivotal ingredient the maximization of entropy. As such, we studied COF and ACOF protocols. Here, feedback enforces a causal direction by allowing information gained to then be imparted into the system. We found that this preference had no effect in an already causal world. However, reversing the causality via ACOF flipped the sign of entropy production, annihilating entropy and reversing the arrow of time.

[1] J J Sakurai. *Modern Quantum Mechanics (Revised Edition)*. Addison Wesley, 1993.

[2] Michael A Nielsen and Issac L Chuang. *Quantum computation and quantum information*. Cambridge University Press, Cambridge New York, 2000.

[3] Udo Seifert. Stochastic thermodynamics, fluctuation theorems and molecular machines. *Reports on Progress in Physics*, 75(12), 2012.

[4] Denis Evans. *Fundamentals of Classical Statistical Thermodynamics*. Wiley-VCH Verlag GmbH & Co. KGaA, Weinheim, Germany, jul 2016.

[5] Kurt Jacobs and Daniel A. Steck. A straightforward introduction to continuous quantum measurement. *Contemporary Physics*, 47(5):279–303, 2006.

[6] K Jacobs. *Quantum Measurement Theory and its Applications*. Cambridge University Press, 2014.

[7] Justin Dressel, Areeya Chantasri, Andrew N. Jordan, and Alexander N. Korotkov. Arrow of Time for Continuous Quantum Measurement. *Physical Review Letters*, 119(22):220507, dec 2017.

[8] C Van Den Broeck. *Stochastic thermodynamics: a brief introduction*. 2013.

[9] Denis J. Evans and Debra J. Searles. Causality, response theory, and the second law of thermodynamics. *Physical Review E*, 53(6):5808–5815, 1996.

[10] Alexander N. Korotkov. Quantum Bayesian approach to circuit QED measurement with moderate bandwidth. *Physical Review A - Atomic, Molecular, and Optical Physics*, 94(4), 2016.

[11] K W Murch, S J Weber, C Macklin, and I Siddiqi. Observing single quantum trajectories of a superconducting quantum bit. *Nature*, 502(7470):211–214, 2013.

[12] Sreenath K. Manikandan and Andrew N. Jordan. Time reversal symmetry of generalized quantum measurements with past and future boundary conditions. *arXiv preprint*, pages 1–24, 2018.

[13] P. M. Harrington, D. Tan, and K. W. Murch. Characterizing a statistical arrow of time in quantum measurement dynamics. *Private communication*, 2018.